ELSEVIER

Journal of Chromatography A, 690 (1995) 29–39

JOURNAL OF CHROMATOGRAPHY A

Origin of peak asymmetry and the effect of temperature on solute retention in enantiomer separations on imprinted chiral stationary phases

Börje Sellergren[a,*], Kenneth J. Shea[b]

[a]*Department of Inorganic and Analytical Chemistry, Johannes Gutenberg University Mainz, Joh.-Joachim-Becherweg 24, D-55099 Mainz, Germany*

[b]*Department of Chemistry, University of California, Irvine, CA 92717, USA*

First received 5 April 1994; revised manuscript received 17 August 1994

Abstract

In enantiomer separations of D- and L-phenylalanine anilide (D,L-PA) on L-PA-imprinted chiral stationary phases (CSPs), the use of an aqueous buffer–organic solvent mixture as mobile phase resulted in improved column efficiency compared with what has previously been observed using mobile phases containing acetic acid as modifier. The dependence of the chromatographic parameters on flow-rate and sample load was studied. A strong dependence of the asymmetry factor (A_s) of the L-form on sample load and a weak dependence on flow-rate indicate that the non-linear adsorption isotherm is the main reason for the broad peaks observed in this system. Depending on the method used for the preparation of the materials, different shapes of the plots of retention and selectivity versus sample load were obtained, indicating differences in the site distribution between the polymers. A slow mass transfer was still present but this was in agreement with results from other ion-exchange separations or separations using large porous particles. The band widths of both enantiomers showed a similar dependence on flow-rate and temperature, which is in contrast to earlier reports on imprinted polymers using reversible covalent bonding in the chromatographic separation. As expected from these results, the separation factor (α) and the capacity factor (k') showed no or only a weak dependence on flow-rate. In a study of the effect of temperature on retention and selectivity, linear Van 't Hoff plots were obtained giving ΔH and $\Delta S'$ values (binding of D- or L-PA, absolute values for the D-form and apparent values for the L-form) and $\Delta\Delta H_{app}$ and $\Delta\Delta S_{app}$ values (differential binding of D,L-PA) that showed an exothermic process. Changing the mobile phase pH from 7 to 4 resulted in an increase, mainly in $\Delta S'$ and $\Delta\Delta S_{app}$. Using an acetic acid-containing mobile phase mixture, an endothermic process was observed with positive ΔH, ΔS, $\Delta\Delta H_{app}$ and $\Delta\Delta S_{app}$ values. The results were interpreted in terms of extensive solvation of the solute ammonium groups, the effect being most pronounced in the acetic acid-containing mobile phase.

* Corresponding author.

0021-9673/95/$09.50 © 1995 Elsevier Science B.V. All rights reserved
SSDI 0021-9673(94)00905-8

1. Introduction

When a solute band passes a chromatographic column it is continuously broadened owing to various dispersion processes [1,2]. These include processes that show little or no flow-rate dependence, such as eddy diffusion or extra-column effects, and flow-rate-dependent processes such as axial diffusion, mass transfer processes including mobile phase, intraparticle and stationary phase diffusion and slow kinetic processes on interaction with the stationary phase. On the other hand, factors such as sample overloading and slow desorption kinetics mainly affect the shape of the peak ([3]; for a review on peak distortion and non-linear chromatography, see Ref. [4]). Altogether these processes counteract the separation of two compounds and lead to lower resolutions. An understanding of their origin is important in order to improve the separations and to gain an insight into the kinetics and mechanism of solute retention. Usually conclusions about the relative importance of these effects can be drawn from chromatographic results at various sample loads, flow-rates and column temperatures. Results from the latter study may further provide valuable information about the energetics of the separation [5–9].

Molecular imprinting is a technique for the preparation of tailor-made chiral stationary phases (CSPs) [10–17]. In our approach, directed non-covalent interactions have been used both in the preparation and in the subsequent evaluation of the phases [12–17]. One enantiomer of the molecule that is the target for the separation is mixed with functionalized monomers in solution (see Fig. 1). The resulting template assemblies are copolymerized with a cross-linking monomer to form a network polymer that can be freed from template by simple extraction. In the chromatographic mode the polymer can then be used for baseline resolution of the original racemic target compound. Mainly owing to the excessive peak broadening observed using these phases, their use for analytical purposes has been limited [12]. Recently we reported on improved chromatographic performance for polymers imprinted with L-phenylalanine anilide (L-PA) using aqueous buffer–organic solvent mobile phase mixtures or after subjecting the polymer to heat treatment [16].

We report here on an attempt to gain a better understanding of the dynamics and energetics controlling the separations on these imprinted phases. First we decided to determine what factors are mainly responsible for the broad and asymmetric peaks in this system. This was followed by a study of the effect of temperature on solute retention and enantioselectivity.

2. Experimental

The imprinted polymers were prepared following a general procedure [16] previously described, by low-temperature photoinitiated free radical polymerization of EDMA (ethylene glycol dimethacrylate) (80 mol%) and MAA (methacrylic acid) (16 mol%) in presence of L-PA (3.8 mol%) as template, using acetonitrile (polymer P1), or methylene chloride (polymer P2) as solvents ($V_{solvent}/V_{total} = 0.57$) (Fig. 1). Prior to work-up of the polymer, P1 was post-treated at 120°C for 24 h.

In the chromatographic evaluation the polymers with a 25–38-μm particle size fraction were slurry packed into 100 mm × 5 mm I.D. stainless-steel columns using as mobile phase MeCN–H_2O–HOAc 92.5:2.5:5, v/v/v). After having passed ca. 50 ml at a flow-rate of 10 ml/min, the columns were equilibrated at 1 ml/min until a stable baseline was reached. Polymer P2 was subjected to thermal treatment by leaving the column overnight in a vacuum oven set at 120°C. Then the column was reconnected to the HPLC system. In the chromatographic studies at variable temperature the columns were immersed in a constant-temperature water-bath together with an additional 50-cm stainless-steel tube connected between the injector and the column. The aqueous buffer–organic mobile phases were acetonitrile (MeCN)–0.05 *M* potassium phosphate (KP) buffer (7:3, v/v). The pH of the buffer was

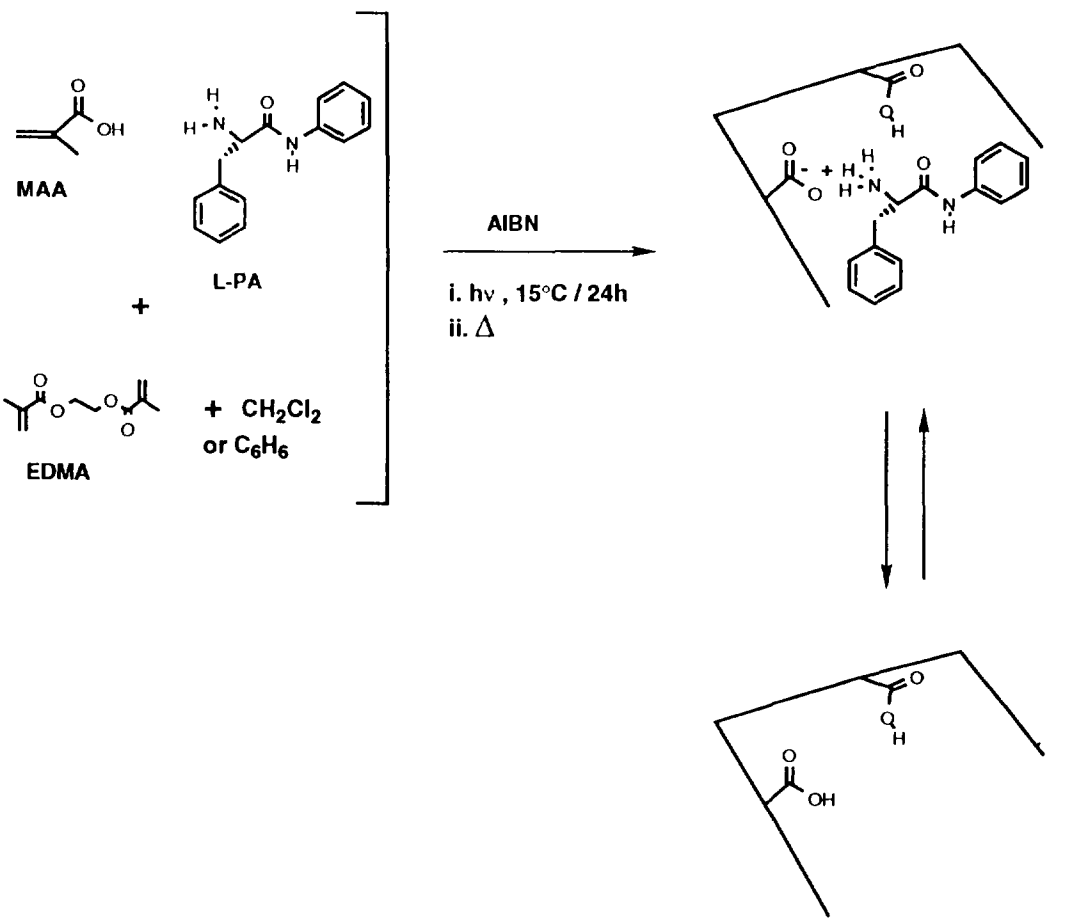

Fig. 1. Preparation of imprinted polymers.

adjusted to 4 or 7 corresponding to a pH of approximately 5 and 8 when measured on the whole system [17].

The capacity factor (k') was calculated as $(t - t_0)/t_0$, where t is the retention time of the solute and t_0 the retention time of a non-retained void marker ($NaNO_3$) (measured to the peak maxima and determined at each temperature). The use of other void markers (acetone, MeCN, HOAc) gave similar results since the solutes were usually retained by more than one void volume. The separation factor (α) measures the relative retention between the enantiomers ($\alpha = k'_L/k'_D$) and the asymmetry factor (A_s) was determined graphically at 10% of the peak maximum as described elsewhere [18]. The reduced plate height (h) was calculated as $h = L/d_pN$, where L = column length, d_p = average particle diameter (32.5 μm) and $N = 5.55(t/t_{1/2})^2$, where $t_{1/2}$ = peak width at half-height, The linear interstitial mobile phase velocity (u) was calculated as $u = F/A\varepsilon$, where F = volumetric flow-rate, A = inner cross-sectional area of column and ε = interstitial porosity (= 0.6), determined as the ratio of the lowest measured void volume (1.2 ml) to the total column volume (2.0 ml). The flow-rate was 1 ml/min, the column temperature 23°C, the volume of solute (D,L-PA, $NaNO_3$ or acetone) injected 10 μl and the UV detection wavelength 260 nm, unless stated otherwise. After the elevated temperature runs a repeat run was performed in order to ensure the stability of the CSP.

3. Results and discussion

3.1. Peak asymmetry and column overload

The peak shape, reflected in the peak asymmetry factor (A_s), is informative about the existence of non-linear binding isotherms and slow adsorption or desorption of solute to the stationary phase. According to Giddings [3], it is possible to distinguish these effects by studying the dependence of A_s on flow-rate and sample load. Thus, if the asymmetry increases with increasing sample load and shows less dependence on flow-rate, the asymmetry is caused mainly by the non-linear binding isotherm. On the other hand, a weak dependence of A_s on sample load and a strong flow-rate dependence are indicative of a slow adsorption/desorption rate. Figs. 2 and 3 show A_s as a function of sample load and flow-rate on two L-PA-selective CSPs prepared by a thermal treatment promoting higher column efficiency [16] (see Experimental). While A_s increases rapidly with increasing sample load, it changes less with flow-rate. Note that the slight decrease in A_s with flow-rate can also be attributed to a non-linear adsorption isotherm [19]. In the same experiment we observed no change in k' and α. The non-linear adsorption isotherm is therefore the main cause of the peak asymmetry. This is reflected in the plots of the capacity factor (k') and separation factor (α) versus sample load (Fig. 4). The shapes of the curves for the two materials are different. Thus k'_L and α on P2 are high with low sample loads but fall off rapidly with increasing sample load to level off above a 10-nmol sample load. On P1, on the other hand, the curves exhibit a small plateau at low sample loads and a less pronounced fall-off at higher sample loads. The corresponding elution profiles on P2 show that the peaks become progressively narrower with increasing sample load (Fig. 5). This is a typical case of an overloaded column with a low plate count where deviation from the "right triangle approximation" [20] is expected to occur [21]. In a study of the binding of 9-ethyladenine to an imprinted polymer [22], the isotherm could be fitted with a Langmuir binary site model composed of a small number of high-energy selective binding sites and a large number of weaker, less selective sites. The corresponding plot of k' versus sample load turns out similar to that obtained for P2 (Fig. 4a), indicating that polymer P2 contains a similar distribution of binding sites. It is noteworthy that a binary site model was also used by Jacobson et al. [23] for

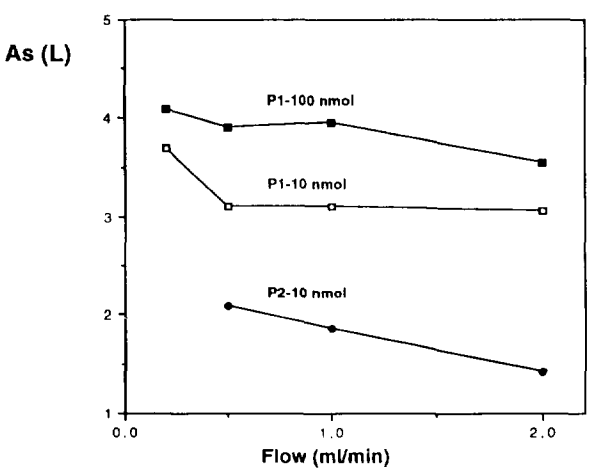

Fig. 2. Asymmetry factor (A_s) versus flow-rate for L-PA at two different sample loads on a column packed with P1 or P2. Mobile phase, MeCN–0.05 *M* KP (pH 7) (7:3, v/v).

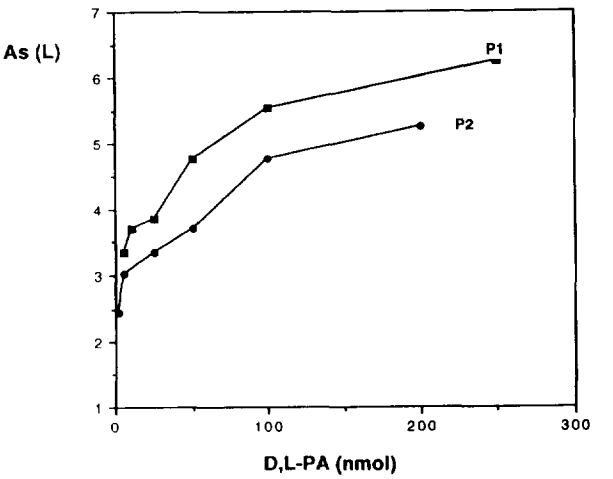

Fig. 3. Asymmetry factor (A_s) of the L-enantiomer versus sample load of D,L-PA on P1 and P2. Flow-rate, 1.0 ml/min; mobile phase, MeCN–0.05 *M* KP (pH 7) (7:3, v/v).

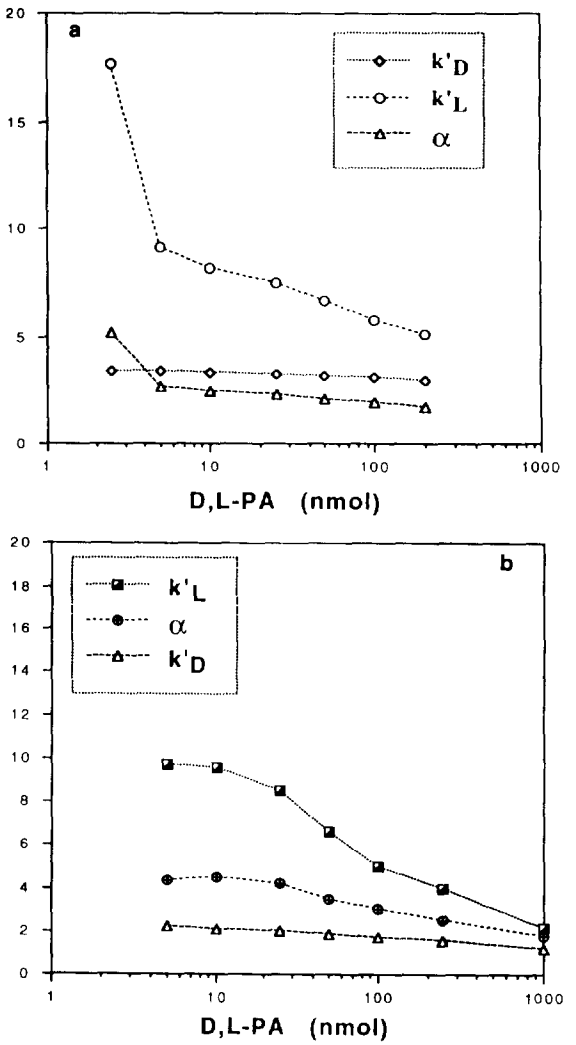

Fig. 4. Capacity factor (k') and separation factor (α) versus sample load of D,L-PA on (a) P2 and (b) P1. Flow-rate, 1.0 ml/min; mobile phase, MeCN–0.05 *M* KP (pH 7) (7:3, v/v).

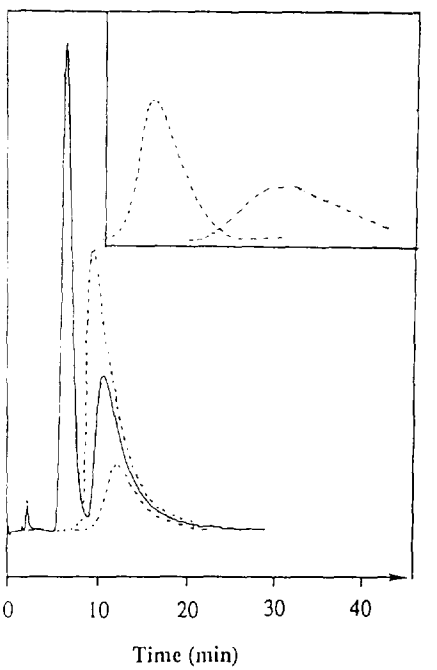

Fig. 5. Elution profiles of increasing loads of D,L-PA applied on P2. Flow-rate, 1.0 ml/min; mobile phase, MeCN–0.05 *M* KP (pH 7) (7:3, v/v). The sample loads from right to left in the chromatogram were 2.5, 5, 50, 100 and 200 nmol. The D-enantiomer is shown only at the 100 nmol sample load.

describing the site distribution in protein-based chiral stationary phases.

What, then, are the possible origins of the different site distributions in the materials? It is noted that P1 and P2 have the same chemical composition but are different only with respect to structure and morphology. This is controlled both by the pore-forming solvent and, by the thermal post-treatment of the materials [16]. Thus, P2 was characterized as gel-like with a low pore volume and surface area but with a relatively high swellability (1.90 ml/ml) that was slightly lower than for the corresponding material not subjected to heat treatment (2.01 ml/ml). P1 was mesoporous with a lower swellabiltiy (1.35 ml/ml), equal to the swellability of the corresponding untreated material. The materials, when not subjected to heat treatment, showed a similar chromatographic dependence on sample load when one was compared with the other [16]. Moreover, higher selectivities and retentions were seen at low sample loads compared with the heat-treated materials. We also found that by subjecting a mesoporous material to heat-treatment in the dry state, that is, the same thermal treatment as used in the preparation of P2, both binding and selectivity were lost. It seems that the structure of the binding sites is more unstable in the porous than in the non-porous materials. Hence a reasonable explana-

tion for the different site distribution in P2 is that unstable and probably highly selective binding sites have been deformed on heat treatment. Apparently these can now stronger bind the D-enantiomer as seen in the higher k'_D values measured on P2 compared with the situation prior to heat treatment. We further note that the saturation capacity of P1 is higher than that of the corresponding material not subjected to heat treatment. This indicates that the heat treatment results in improved site accessibility. Obviously, more detailed studies on the effect of heat treatment need to be carried out, including measurements of the complete binding isotherms [4].

3.2. Peak dispersion

As the retention of the complementary solute (L-PA) on the imprinted polymers follow a non-linear binding isotherm as indicated from the plots of k' versus sample load (Fig. 4), the resulting peaks are asymmetric (see Fig. 5) and the theoretical models describing the various dispersion processes are not applicable [1,2]. On P2, the column efficiency improved at higher temperature (Fig. 6) but with little effect on peak asymmetry. Nevertheless, the bands of the less retained enantiomer (D-PA) and of the void marker, acetone, are fairly gaussian (see Fig. 5) and their retention time changes marginally with sample load. The associated band widths are therefore expected to be mainly a result of the band-broadening mechanisms that are considered in the models. Previously we showed that the solute retention on this type of CSP can be accurately described by a theoretical model for weak cation exchange [17].

In Fig. 7, double logarithmic plots of reduced plate height (h) versus linear mobile phase

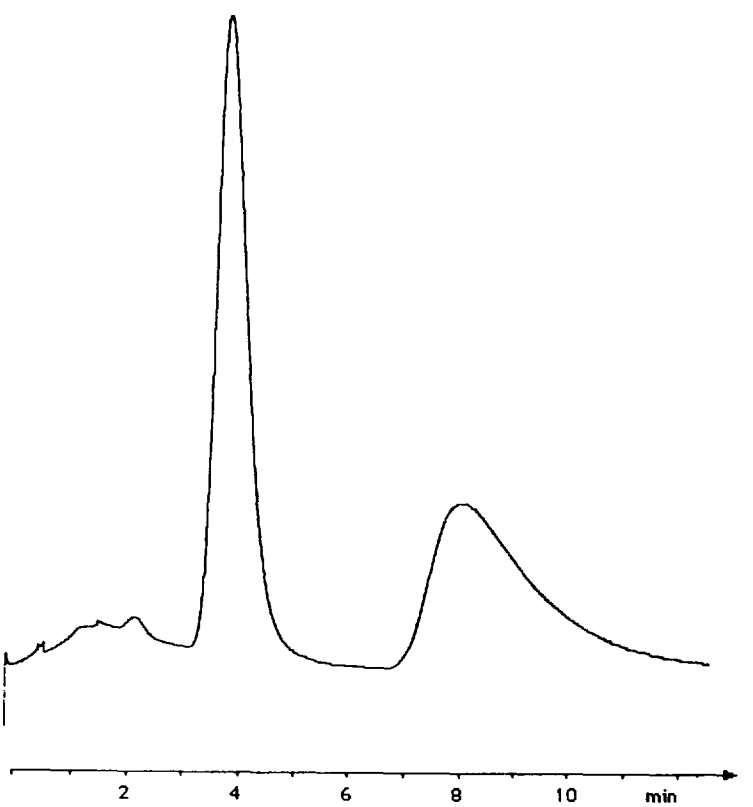

Fig. 6. Elution profile of D,L-PA (10 nmol) applied on P2. Flow-rate, 1.0 ml/min; mobile phase, MeCN–0.5 *M* KP (pH 4) (7:3, v/v); column temperature, 60°C. The reduced plate heights were $h_D = 12$ and $h_L = 35$.

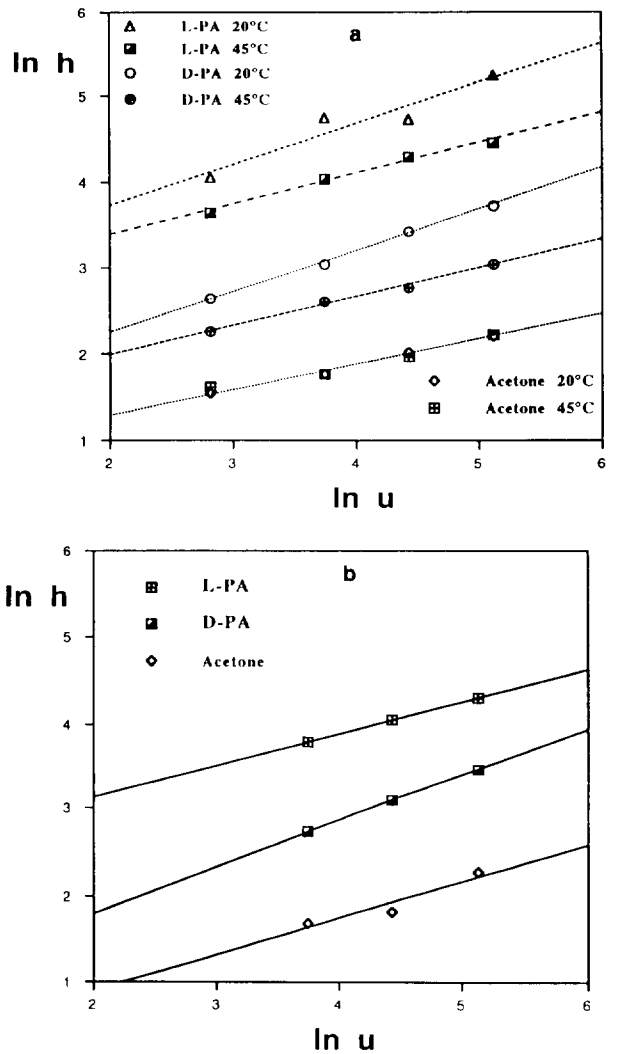

Fig. 7. Double logarithmic plot of reduced plate height (h) versus linear mobile phase velocity (u) in the chromatography of D,L-PA (100 nmol) on (a) a polymer prepared using benzene as porogen at two different column temperatures: at 20°C, $k'_1 \approx 6$, $k'_2 \approx 2.5$, and at 45°C, $k'_1 \approx 2.1$, $k'_2 \approx 1.0$; (b) polymer P2 at 20°C. Mobile phase, MeCN–0.05 M KP (pH 7) (7/3, v/v).

velocity (u) are shown for D- and L-PA and the non-retained acetone marker on polymer P2 and a polymer prepared using benzene as porogen. Note that the data for the L-enantiomer have been included for comparative purposes. The plots are all linear and the slope changes with temperature in agreement with other types of ion-exchange separations using porous particles [24–26]. The mass transfer here was believed to be limited by a slow intraparticle diffusion. In this context we note that the plots of acetone do not change with temperature, indicating that the mobile phase diffusion of the neutral void marker is not limiting the mass transfer.

Although the peak of the L-enantiomer is strongly asymmetric, it is interesting that the plots are essentially parallel with those of the D-form. Together with the small change in relative plate heights with temperature (data not shown), this indicates that the enantioselective resistance to mass transfer is small at this sample load (100 nmol). This should be compared with the strongly temperature-dependent relative plate heights observed in the separation of sugar enantiomers on imprinted polymers based on reversible boronate ester formation [11].

3.3. Effect of temperature

Chromatographic retention data from variable-temperature runs may be used to estimate thermodynamic properties according to the well known Van 't Hoff relation [5–9]:

$$\ln k' = -\Delta H/RT + \Delta S/R + \ln \phi \quad (1)$$

where ϕ = phase volume ratio and R = gas constant. Thus linear portions of these plots give enthalpies (ΔH) and entropies (ΔS) of the solute adsorption from the slope and intercept, respectively. The ΔH and ΔS values thereby obtained can rarely be ascribed to a single process but are rather a complex combination of various contributions such as solute–site solvation and desolvation, the unsolvated solute–site interaction, solvation of bound solute, conformational changes, multiple equilibria and mixed retention mechanisms [1]. By plotting $\ln \alpha$ ($\alpha = k'_L/k'_D$ = separation factor) versus $1/T$, all processes that do not contribute to the enantiomeric discrimination cancel out and information about the energetics of the separation can be obtained from

$$\ln \alpha = -\Delta\Delta H/RT + \Delta\Delta S/R \quad (2)$$

The dependence of the chromatographic parameters on temperature were investigated in three different solvent systems. Based on the stable α and k' values obtained on P2 with

respect to flow-rate (at a sample load of 100 nmol at pH 7, the retention data were $k'_L = 4.21 \rightarrow 4.25$ and $\alpha = 1.52 \rightarrow 1.54$ for a flow-rate increase from 0.5 to 2 ml/min; at pH 4 and in the HOAc-containing mobile phase, however, a slight decrease in k'_L and α was observed: pH 4, $k'_L = 3.93 \rightarrow 3.40$ and $\alpha = 3.10 \rightarrow 2.70$; HOAc, $k'_L = 11 \rightarrow 8$ and $\alpha = 6.5 \rightarrow 5.8$; for a flow-rate increase from 0.2 to 2 ml/min), we considered that a discussion of the thermodynamic behaviour of this phase would be justified. For the D-enantiomer the linear isotherm, as indicated by the stable k' values in Fig. 4a, allows thermodynamic quantities to be determined. For the L-form, however, the contribution from thermodynamic band broadening only allow qualitative conclusions. Nevertheless, as the sample load between 10 and 100 nmol had little influence on the corresponding Van 't Hoff plots, the slope and intercept were determined giving values assigned as apparent thermodynamic quantities (ΔH_{Lapp} and ΔS_{Lapp}).

Figs. 8–10 show the plots of ln k' versus $1/RT$ at a mobile phase pH of 7 and 4 and in a mobile phase containing acetic acid as additive [MeCN–H_2O–HOAc (92.5:2.5:5)]. In the latter instance, a larger sample load had to be applied (100 nmol) because of the excessive peak broadening of L-PA. At pH 7 a linear dependence of ln k' on $1/RT$ is seen with decreasing k' with increasing temperature. On lowering the pH to 4, a non-linear plot is obtained with a linear portion at higher temperature. The linear portions of these plots were fitted by least-squares linear regression analysis, giving ΔH and $\Delta S'$ values (for the

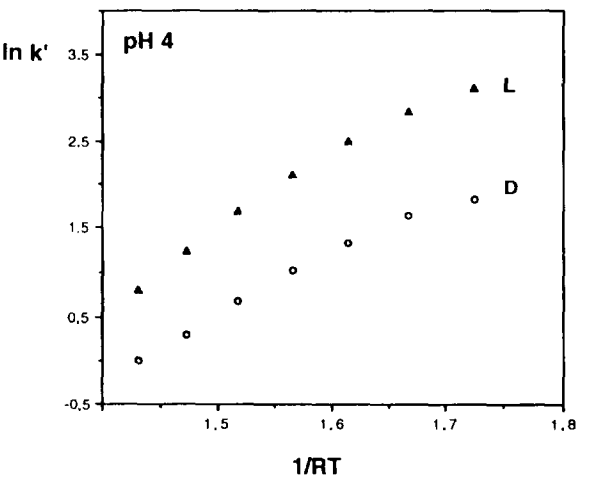

Fig. 9. Van 't Hoff plot as in Fig. 8 but at pH 4. The column temperature was increased from 20 to 80°C in 10°C increments.

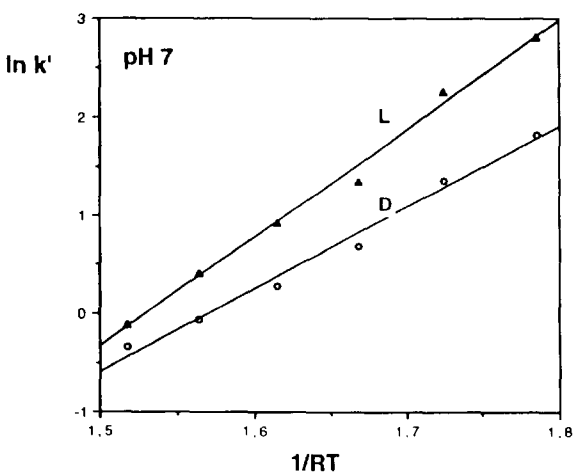

Fig. 8. Van 't Hoff plots of the capacity factors (k') for 10 nmol of D,L-PA chromatographed on P2. Mobile phase, MeCN–0.05 *M* KP (pH 7) (7:3, v/v). The column temperature was increased from 10 to 60°C in 10°C increments.

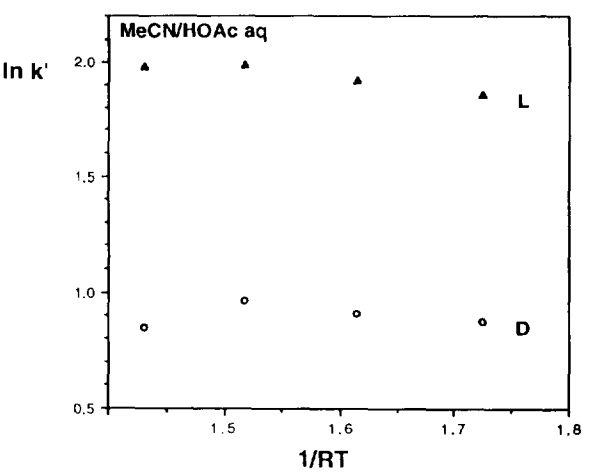

Fig. 10. Van 't Hoff plots of the capacity factors (k') for D- and L-PA (100 nmol) on an L-selective polymer. Mobile phase, MeCN–H_2O–HOAc (92.5:2.5:5). The column temperature was increased from 20 to 80°C in 20°C increments.

Table 1
Chromatographic determination of enthalpies and entropies of binding of D- and L-PA to an L-PA-imprinted polymer (P2) from the data in Figs. 8–11

Mobile phase	D,L-(nmol)	ΔH_D (kcal/mol)	$\Delta H_{L,app}$ (kcal/mol)	$\Delta S'_D$ (cal/mol · K)	$\Delta S'_{L,app}$ (cal/mol · K)	$\Delta\Delta H_{D,L,app}$ (kcal/mol)	$\Delta\Delta S_{D,L,app}$ (cal/mol · K)
MeCN–H_2O–HOAc (92.5:2.5:5)	100	0.43	0.64	3.2	5.9	0.47	3.5
MeCN–0.05 *M* KP (pH 4) (7:3)	10	−7.6	−9.9	−22	−26	−1.7	−3.1
	100	−7.0	−9.0	−20	−25	−1.7	−3.6
MeCN–0.05 *M* KP (pH 7) (7:3)	10	−8.4	−11	−26	−34	−2.7	−7.6
	100	−9.4	−11	−30	−35	−1.7	−4.8

The enthalpies (ΔH) and entropies (ΔS) (absolute values for the D-enantiomer and apparent values for the L-enantiomer) were obtained from linear regression of the linear portion of corresponding Van 't Hoff plots of ln k versus $1/RT$. The $\Delta\Delta H_{app}$ and $\Delta\Delta S_{app}$ values were obtained from ln α versus $1/RT$. These plots were apparently linear throughout the temperature interval used in the study. The plots had a correlation factor of at least 0.96. $\Delta S' = \Delta S + R \ln \phi$, where ϕ = column phase volume ratio. 1 cal = 4.184 J.

L-form only apparent values) as shown in Table 1 at two different sample loads. On changing from pH 7 to pH 4, ΔH and $\Delta S'$ increase. As protonation of the solute occurs in this pH interval, a major change in solvation–desolvation effects affecting the separation is to be expected. Interactions requiring desolvation of extensively solvated species are usually associated with a more positive entropy term than the corresponding non-solvated interactions. This effect can be expected for interactions between solvated ammonium and carboxylate groups. Note that aqueous solvation of ammonium ions is strong and can involve four shells of water molecules with a $\Delta H°$ of 30–80 kcal/mol [27]. The solvation of the solute at pH values below its pK_a value (pK_a = 5.4 in this solvent system) [17] is thus likely to have a major influence on the binding process. Apparently solvation is even more pronounced using the organic–acetic acid mobile phase, reflected in the positive values of both ΔH and $\Delta S'$. This is in agreement with our earlier study on the stability of complexes formed between methacrylic acid and L-PA prior to polymerization and between acetic acid and L-PA in the mobile phase [14]. It should be noted that such a rare type of chromatographic temperature dependence was recently observed also in the separation of chiral amines on chiral crown ethers [28]. The endothermic behaviour here was also explained by solute desolvation on formation of electrostatic interactions between the site and the solute.

From the plots in Fig. 11, $\Delta\Delta H_{app}$ and $\Delta\Delta S_{app}$, describing the enantioselective contribution to

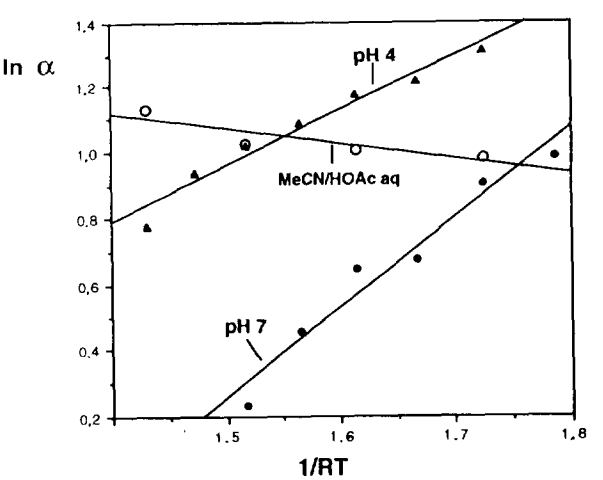

Fig. 11. Van 't Hoff plots of the separation factor (α) for the experiments described in Figs. 8–10. Using the HOAc-containing mobile phase, the amount applied was 100 nmol.

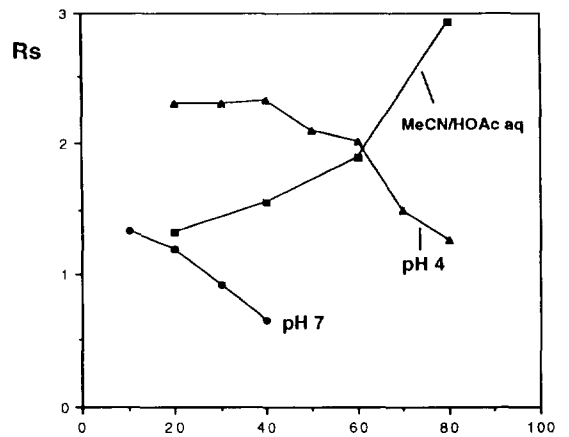

Fig. 12. Resolution factor (R_s) versus column temperature for the experiments in Figs. 8–11.

binding (see Table 1), were calculated. Similar trends are observed here as in the plot of ln k'. Thus $\Delta\Delta S_{app}$ and to some extent $\Delta\Delta H_{app}$ increase with decreasing pH. Again, these changes can be attributed to solvation–desolvation phenomena. At low pH the ammonium ions of the solute are strongly solvated. On binding to the negatively charged sites, the most strongly bound enantiomer will require more desolvation than the antipode, which may bind to the sites while still being partly solvated. In the acetic acid-containing mobile phase this effect is apparently important enough to cause an endothermic behaviour. At pH 7, however, most of the solute is deprotonated and thus less strongly solvated [27]. The polymer is abundant in non-ionized carboxylic acid groups [17]. Hence interactions between non-ionized solute and non-ionized sites, a process likely to involve less solvation–desolvation of the interacting species, may account for the lower $\Delta\Delta S_{app}$ and slightly lower $\Delta\Delta H_{app}$ found at pH 7. The temperature effects are clearly reflected in the dependence of resolution (R_s) on temperature. Whereas at pH 7 an increase in temperature leads to a decrease in resolution, the other extreme is seen using the acetic acid-containing mobile phase, namely an increase in R_s with increase in temperature (Fig. 12).

4. Conclusions

The present results indicate that the peak asymmetry in a buffered mobile phase system is mainly due to the non-linear binding isotherm resulting in a continuous overloading of sites. The site distribution depends on the method used in the preparation of the materials where various heat treatments can be applied in order to change the binding site distributions or accessibility. Kinetic factors such as slow solute adsorption or desorption appears to be of less importance, although mass transfer limitations are still present. At pH 7, the dependence of the plate height for the least retained enantiomer (gaussian peak) on the mobile phase velocity was similar to those commonly observed in ion-exchange separations. Neither the retention nor selectivity changed here with variations in flow-rate. It should be noted that polymers imprinted by reversible boronate ester formation showed a different chromatographic behaviour [10]. The separation factor and retention increased significantly here with decreasing flow-rate whereas the plate number remained essentially constant. The mass transfer was believed to be limited by a slow, reversible, covalent binding step while the diffusional limitations were assumed to be negligible.

A temperature study on the phases led to Van 't Hoff plots that were strongly dependent on the mobile phase pH and also on the mobile phase composition. From linear portions of these plots values of ΔH and $\Delta S'$ (absolute for the D-enantiomer and apparent for the L-enantiomer) for the retention and $\Delta\Delta H_{app}$ and $\Delta\Delta S_{app}$ for the separation could be calculated. The exothermicity of both the retention and the separation decreases with decrease in pH and an endothermic process is observed when using an organic–acetic acid mobile phase. These effects were believed to be caused mainly by the desolvation required on interactions between

strongly solvated ammonium and carboxylate groups.

Acknowledgements

This work was supported by grants from the Swedish Natural Science Research Council and from the US National Science Foundation. Financial support from Lars Hiertas Minne is gratefully acknowledged.

References

[1] G.S. Weber and P.W. Carr, in P.R. Brown and R. Hartwick (Editors), *High Performance Liquid Chromatography*, Wiley-Interscience, New York, 1989, pp. 1–15.
[2] J.Å. Jönsson (Editor), *Chromatographic Theory and Basic Principles*, Marcel Dekker, New York, 1987.
[3] J.C. Giddings, *Anal. Chem.* 13 (1963) 1999.
[4] A.M. Katti and G.A. Guichon, *Adv. Chromatogr.*, 31 (1992) 1–119.
[5] W.R. Melander, B.-K. Chen and C. Horvath, *J. Chromatogr.*, 185 (1979) 99–109.
[6] W.R. Melander, J. Stoveken and C. Horvath, *J. Chromatogr.*, 185 (1979) 111–127.
[7] W.R. Melander, A. Nahum and C. Horvath, *J. Chromatogr.*, 185 (1979) 129–152.
[8] A. Nahum and C. Horvath, *J. Chromatogr.*, 203 (1981) 53–63.
[9] W.H. Pirkle, *J. Chromatogr.*, 558 (1991) 1–6.
[10] G. Wulff and W. Vesper, *J. Chromatogr.*, 167 (1978) 171.
[11] G. Wulff and M. Minárik, *J. High Resolut. Chromatogr. Chromatogr. Commun.*, 9 (1986) 607.
[12] For a review, see B. Sellergren, in G. Subramanian (Editor), *Chiral Separations by Liquid Chromatography*, VCH, Weinheim, 1994, pp. 69–93.
[13] B. Sellergren, B. Ekberg and K. Mosbach, *J. Chromatogr.*, 347 (1985) 1.
[14] B. Sellergren, M. Lepistö and K. Mosbach, *J. Am. Chem. Soc.*, 110 (1988) 5853.
[15] M. Lepistö and B. Sellergren, *J. Org. Chem.*, 54 (1989) 6010–6012.
[16] B. Sellergren and K.J. Shea, *J. Chromatogr.*, 635 (1993) 31–49.
[17] B. Sellergren and K.J. Shea, *J. Chromatogr.*, 654 (1993) 17–28.
[18] L.R. Snyder and J.J. Kirkland (Editors), *Introduction to Modern Liquid Chromatography*, Wiley, New York, 1979, pp. 234–237.
[19] J.H. Knox and G. Vasvari, *J. Chromatogr.*, 83 (1973) 181–194.
[20] J.H. Knox and H.M. Pyper, *J. Chromatogr.*, 363 (1986) 1.
[21] L.R. Snyder, G.B. Cox and P.E. Antle, *Chromatographia*, 24 (1987) 82–96.
[22] K.J. Shea, D.A. Spivak and B. Sellergren, *J. Am. Chem. Soc.*, 115 (1993) 3368–3369.
[23] S. Jacobson, S. Golshan-Shirazi and G. Guichon, *J. Am. Chem. Soc.*, 112 (1990) 6492.
[24] J.F.K. Huber, *Ber. Bunsenges. Phys. Chem.*, 77 (1973) 179.
[25] A. Jardy and R. Rosset, *J. Chromatogr.*, 83 (1973) 195–204.
[26] R. Eksteen, J.C. Kraak, P. Linssen, *J. Chromatogr.*, 148 (1978) 413–427.
[27] M. Meot-Ner, in J.F. Liebman and A. Greenberg (Editors), *Molecular Structure and Energetics*, Vol. 4, VCH, Weinheim, 1987, p. 71.
[28] R. Kuhn, F. Erni, T. Bereuter and J. Häusler, *Anal. Chem.*, 64 (1992) 2815–2820.